

# Design and test of the ion mobility spectrometer with corona discharge ion source

J.Husárik, M.Stano, J.D.Skalný, M. Tabrizchi<sup>a</sup> and Š. Matejčík

*Department of Experimental Physics,  
Faculty of Mathematics, Physics and Informatics, Comenius University,  
Mlynská dolina F2, 84248 Bratislava, Slovakia*

*<sup>a</sup>Chemistry Department, Isfahan University of Technology,  
Isfahan 84154, Iran*

## Abstract

In present paper we describe in detail the design and construction of a home built ion mobility spectrometer with corona discharge as an ionization source. The ion mobility spectra have been recorded using the corona discharge in two different modes: i) chemical ionization and ii) direct ionization in the corona discharge. The chemical ionization of the organic compounds resulted in less fragmented ion mobility spectra in comparison to the direct ionization of the compounds in the corona discharge. The measured positive ion mobility spectra of several organic compounds including acetone, methanol, ethanol and benzene are presented.

# 1 Introduction

The Ion Mobility Spectrometry (IMS) is an ion separation method, based on the phenomenon that different ion have different drift velocities in an inert drift gas and homogeneous electric field. The drift velocity under such conditions is given by the formula  $v_d = K \cdot E$ , where  $K$  is the ion mobility [ $\text{V}\cdot\text{s}^{-1}\cdot\text{m}^{-2}$ ] and  $E$  is the intensity of the electric field. The the ion mobility can be expressed also by the formula:

$$K = \frac{l_d}{t_d \cdot E} \quad (1)$$

where  $l_d$  is the length of the drift tube and  $t_d$  is the drift time of the ions. As the mobility depends on the collisions of the ions with the drift gas it depends also on the density of the drift gas. Therefore a correction to the standard conditions (273 °K, 101kPa) is made and resulting value is reported as reduced mobility  $K_0$  given by formula

$$K_0 = K \cdot \frac{273}{T} \cdot \frac{p}{101} \quad (2)$$

The IMS technique has been developed and introduced in 1970 [1, 2] under the name plasma chromatography. Since then a variety of different devices working on this principle was developed, mainly for detection of drugs [3], explosives and chemical weapons [4, 5, 6]. The advantages of the ion mobility spectrometry are the high sensitivity, low cost, small size and absence of the vacuum system. Thanks to these properties the IMS technique is widely used as an excellent detector for dangerous substances. In the 80's a huge progress was achieved on the field of the ion - molecule reactions at atmospheric pressure and the IMS was rediscovered as a powerful analytical method [7, 8]. However, the commercially used IMS were often single purpose only and are not suitable for the scientific needs. Such

an instrument has low variability and its use is limited. For this reason we have decided to develop our ion mobility spectrometer.

Generally, the IMS consists of several parts. It is the ionization source, the reaction region, the shutter grid and the drift tube. The most common ionization source is  $^{63}\text{Ni}$  ( $\beta$ -radiation) radioactive source, which is suitable for many applications because of its stability, low cost and low weight. Unfortunately, this source is radioactive and there is tendency to replace the radioactive source from environmental reasons. Several ionization sources using the UV ionization [9, 10], the multi-photon laser ionization [11], the electrospray ionization [12] or the corona discharge [13] were tested in the past. The corona discharge ionization source was used for detection of aromatic compounds and alkanes, which are not detectable by conventional IMS. The ionization efficiency of such a source is very high and it can be used for production as the positive ions so the negatively charged ions. The corona discharge source can be operated in two basic modes.

In the first mode the sample gas is introduced direct into the corona discharge. The direct ionization in the corona discharge, which includes such reactions like electron induced ionization, field ionization by the high electric fields, electron attachment and subsequent ion - molecule reactions result in strong fragmentation of the molecules and complicated IMS spectra. If the ionization source is working in the second mode, the corona discharge burns in the drift gas (usually nitrogen) and the primary ions are formed from the working gas. The ionization of the sample gas occurs in a different part in the reaction region. The primary ions (usually  $\text{NH}_4^+$ ,  $\text{H}_3\text{O}^+$ ...) enter the reaction region and take part in the ion - molecule reactions with the sample gas. The ionization of the sample gas proceeds via proton transfer reactions. This type of ionization is called chemical, or soft ionization.

The positive ions are mainly produced by the proton transfer reactions depending on

the proton affinity of the compounds or by clustering. In order to predict the possible products of the reactions, it is necessary to identify the primary ions produced by the ion source without the presence of the sample. Several works have been published on this topic [14, 15, 16] and following ions  $\text{H}_3\text{O}^+$ ,  $\text{H}^+ \cdot (\text{H}_2\text{O})_n$ ,  $\text{NO}^+ \cdot (\text{H}_2\text{O})_n$  and  $\text{NH}_4^+ \cdot (\text{H}_2\text{O})_n$  have been observed using nitrogen as the working gas. It is expected, that the ion  $\text{NH}_4^+$  comes from the impurities in the apparatus.

## 2 Experimental setup

The ion source in the present IMS is based on the corona discharge (Figure 1) in point to plane geometry. The discharge chamber is made of teflon cylinder with 50 mm inner diameter. A grid in the form of parallel tungsten wires (diameter 100  $\mu$  m) with relative distance of 1 mm represents the plain electrode of the corona discharge. The point electrode is made of tungsten wire (diameter 50  $\mu$  m) which is mounted in a ceramic tube located in the axis of the discharge chamber. The role of this tube is to hold the point electrode in the required position and it also serves as a gas inlet. The distance between the tip of the wire and the plain electrode can be adjusted by moving the ceramic tube along the axis of the discharge chamber.

In order to achieve the maximal ion current was the point to plane distance varied in the range 3 - 12 mm. In the positive corona the maximal current was observed at 4 mm point to plane distance and the ignition voltage was in the range 2-2,5 kV. The maximal ion current is limited by the recombination of ions on the plane electrode (corona grid). The ratio of the ions caught by the grid to the ions that pass the grid is proportional to the ratio  $E_2/E_1$ , where  $E_1$  is the intensity of electric field in the drift tube and  $E_2$  is the intensity of electric field in the discharge chamber.

The reaction region (Figure 2) consist of several parallel ring electrodes, separated by teflon seals. The length of the reaction region can be varied, depending on number of used electrodes. The first electrode in the reaction region is specially designed and its function is to avoid the diffusion of the sample gas into the discharge chamber. Two ports for the gas inlet and for the gas outlet are build into this electrode. The rest of the electrodes has the standard dimensions identical with the electrodes used in drift tube. Inner diameter

of the ring electrode is 50 mm and the length of the electrode is 9 mm. All electrodes are connected to voltage divider.

An electric shutter grid (Figure 3) is placed at the end of the reaction region. The shutter grid is one of the most important parts of the IMS. Its role is to keep the ions in reaction region and to inject the ions into the drift region. The grid is made of parallel wires, located in one plane perpendicular to the axis of the spectrometer. The wires are on the electric potential  $V_d \pm V_{sg}/2$ , where  $V_d$  is the potential of the drift tube at the position of the shutter, and  $V_{sg}$  is closing potential between neighboring wires. This potential creates an electric field perpendicular to the electric field formed by the drift tube. As the ions follow electric field, they hit the grid wires and loose their charge due to recombination processes. If a short circuit is created between the grid wires then the electric potential of the wires is  $V_d$  and there is no perpendicular electric field generated by the grid, the shutter is opened. The ions are able to enter the drift region.

The construction of the shutter grid may influence the resolution and sensitivity of the spectrometer. This is due to the influence of the perpendicular electric field to the drift electric field. The consequential electric field surrounding the grid is given by superposition of this two fields. If the perpendicular field is to strong the gate depletion effect occurs. If the perpendicular field is to weak, the fast ions can penetrate into the drift region even if the gate is closed. A constant background in the spectra is observed in this case. The proper value of the shutter grid electric field is in the factor from 1 to 10 of the electric field in the drift tube.

The role of the drift tube is to separate the ions according to their individual mobilities, so a homogeneity of the electric field in this part is required. The drift tube consists of identical brass rings separated by the teflon rings. The inner diameter of the ring is 50 mm

and the length is 9 mm. The distance between two rings is 1 mm. The length of the drift region can be varied using different number of the rings. The drift region is ended with ion collector. The ion collector consist of aperture grid, collector and shielding. The collector is made of brass and its diameter is 2 cm in order to detect only ions drifting close to the axis of the apparatus. The collector is shielded from the front side by an aperture grid and from other sides by a brass body. The aperture grid is made of parallel Wolfram wires, 75  $\mu\text{m}$  thick and 1 mm apart of each other. The distance from the collector to the aperture grid is 1 mm.

The sensitivity of the IMS is high and even a small amounts of impurities could cause a contamination of the apparatus. The contamination of the spectrometer result in difficulties in interpretation of the ion spectra. High requirements are imposed on the gas inlet system (Figure 4). The gas inlet system is made of teflon in combination with stainless steel. The working gas used in present experiment was  $\text{N}_2$  with purity 5.0. The working gas is additionally dried by zeolites. The dried gas is divided into 3 branches: drift gas, corona gas and the carrier gas. The drift gas enters the apparatus at the end of the drift tube and flows in the opposite direction as the drifting ions. Its role is to clean the drift tube. The corona gas is introduced into the corona region and the flow of this gas decreases the diffusion of the sample into the corona region. The role of the carrier gas is to import the sample into the reaction region. The sample (a vapor, or a gas) is injected into the carrier gas using a syringe. A specialized injection port is placed in the gas system. The gas flow rates were controlled by flow meters and regulated by adjustable valves. In order to achieve clean and stable conditions, the whole system is heated. The temperature of the IMS can be controlled in the temperature range 20 - 150  $^\circ\text{C}$ .

Two high voltage power supplies were used in the IMS. One power supply serves for the

corona discharge. In order to limit the discharge current a  $1,5\text{ M}\Omega$  resistor was connected in the series with the discharge. The second power supply is connected to the voltage divider and supplies the drift tube with a homogeneous electric field. The shutter grid is opened and closed by a high voltage switch. The HV switch is controlled electronically by a pulse generator. The oscilloscope is synchronized with the puls generator. Opening time of the shutter grid can be varied in range  $50 - 500\ \mu\text{s}$  and the opening frequency in range  $20 - 40\ \text{Hz}$ .

The ion current measured on the collector plate is amplified by a current-to-voltage amplifier with ratio  $1\ \text{nA} \sim 10\ \text{mV}$ . The amplified signal is averaged by an digital oscilloscope and the results are stored by a computer.

### 3 Results and Discussion

The measurements of the ion mobility spectra presented in this paper have been performed under following experimental conditions (Table 1):.

In our first measurements we have studied the ion formation in the corona discharge in pure nitrogen gas. A typical primary ion spectra is shown in the figure 6. The relative positions of the peaks in the spectra indicate that the first peak originates from  $\text{NH}_4^+ \cdot (\text{H}_2\text{O})_n$  and the second peak from  $\text{H}_3\text{O}^+$ .

We have introduced trace amount of  $\text{NH}_4\text{OH}$  into the discharge (7). From this molecule the  $\text{NH}_4^+$  is preferably formed in the corona discharge and we have observed increase of the first peak. This confirmed our hypothesis that the first peak correspond to the  $\text{NH}_4^+$  and  $\text{NH}_4^+ \cdot (\text{H}_2\text{O})_n$  ions. A similar method was used to identify the second peak. However, after introducing water vapor into the discharge, again a increase of the first peak was observed. This effect is well known and is present due to trace amounts of the ammonia in the water.

Because the speed of the reaction depends on the concentration of reactants therefore the high concentration of the water clusters caused an increase in production of the  $\text{NH}_4^+$ . The proton affinity of  $\text{NH}_3^+$  (9 eV) is higher then the proton affinity of the water molecule (7,2 eV) and most of the ions  $\text{H}_3\text{O}^+$  are converted to the  $\text{NH}_4^+$  ions. The  $\text{NH}_3$  is present in small concentrations in the ambient air and is very difficult to remove it from the spectrometer.

More compounds were added into the corona discharge in order to determine the ions corresponding to the third peak. The results of this measurements did not give a solution and additional experiments are needed to explain the nature of these peaks.

We have carried out experiments in order to study formation of the positive ions from some organic molecules i) via ion-molecule reaction of the molecules with the primary ions (chemical ionization) ii) directly in the the corona discharge and. These measurements should indicate the difference between these two ionization methods.

As the first molecule the acetone has been studied. The ion -mobility spectra of acetone are presented in the Figure 8. In the case of the chemical ionization a simple mobility spectra was expected (Figure 8 a). The sensitivity of the apparatus in this operation mode was lower and the shutter grid opening time had to be set to a higher value. This step was necessary to get sufficient signal, but it causes a decrease of the resolution. In the future we plan to increase the ion production in the case of chemical ionization in order to get also in this case better resolution. In the case of direct ionization in the corona discharge (Figure 8 b), the sample was permitted to enter the corona region and the sample ionizes also in the discharge. The products of dissociation processes and also subsequent ion-molecule reactions are expected to be present in the mobility spectra. The corona discharge ionization measurements were performed at higher temperature in comparison to the chemical ionization so the drift times in the b) spectra are shorter. A number of different organic compounds (Table 2) was chosen to investigate differences between the chemical and direct ionization in the corona discharge.

A low level of dissociation of acetone in corona discharge is most probably due to the fact that the fragment ions formed in the corona discharge are effectively converted via series of ion-molecule reaction into the protonated acetone ion and thus the fragment ion are not present in the spectra. Similar situation occurs also in the ethanol (Figure10.) However, a huge decrease of signal is observed in spectra a), referring to processes between primary ions and the sample. The second peak in a) spectra is possibly a sum of two

signals corresponding to  $\text{H}_3\text{O}^+$  and ethanol ion. This assumption is based on the position of these peaks in the spectra b).

Significant differences between chemical ionization and direct corona discharge ionization have been observed in the spectra of benzene (Figure 11). The major peak in spectra b) has corresponding mobility  $2,84 \text{ cm}^2 \cdot \text{V}^{-1} \cdot \text{s}^{-1}$  and such ion peak is not present in the spectra a). It might be a fragment of benzene or a result of an ion-molecule reaction of the fragment with other molecules in the reaction region. The benzene parent ion has the mobility around  $2,58 \text{ cm}^2 \cdot \text{V}^{-1} \cdot \text{s}^{-1}$  and it was observed in spectra a).

An ion with reduced mobility of about  $2,4 \text{ cm}^2 \cdot \text{V}^{-1} \cdot \text{s}^{-1}$  was also observed. If we consider, that no dissociation processes take place in the case of chemical ionization, the ion can be identified as a benzene dimer. Methanol (Figure 9) spectrum is not resolved good enough and the intensity of the parent ion is too weak for a further analysis. This might be caused by relative low proton affinity of these compounds.

The information obtained from the ion mobility spectra of organic compounds is still not sufficient. The assignment of the particular peaks to the ionic structures is still difficult, because there still do not exist reliable databases of reduced mobilities of the ions. For this reason it is very useful to combine the IMS with a mass spectrometer. However, present measurements have shown that the parameters of the home build IMS spectrometer are very good. Additionally, significant difference between the chemical ionization and the direct ionization of the molecule in corona discharge was observed. The chemical ionization in combination with IMS is an useful non destructive ionization method. The sensitivity, resolution and simplicity of the corona discharge ionization are good attributes for the needs of fast detection. Also the corona discharge might be investigated using this method.

## 4 Conclusions

In the present paper we have presented the design of the ion mobility spectrometer built at Comenius University and the first test measurements obtained with this spectrometer. The first results indicates that the spectrometer has very good performance, which is comparable with other instruments. Present study also showed that the corona discharge ion source is very effective source of the positive ions for the IMS delivering stability and high intensities of the ions. Moreover, according to the requirements of the experiment the corona discharge could be operated in two different modes delivering either strong fragmented ions or unfragmented protonated ions.

## 5 Acknowledgment

This work was supported by the Slovak grant agency project Nr. APVT-20-007504.

## References

- [1] M. J. Cohen and F. W. Karasek, *J. Chromatogr. Sci.* 8, 330, (1970)
- [2] F. W. Karasek, *Res. Dev.* 21, 34, (1970)
- [3] T. Keller, Akihiro Miki, Priska Regenscheit, Richard Dirnhofer, Andrea Schneider and Hitoshi Tsuchihashi; *For. Sci. Intern.*, 94, 1-2, (1998), 55-63
- [4] Igor A. Buryakov; *J. Chromatogr. B*, 800, 1-2, (2004), Pages 75-82
- [5] Gavin A. Buttigieg, Andrew K. Knight, Stephen Denson, Carolyn Pommier and M. Bonner Denton; *For. Sci. Intern.*, 135, 1, (2003), 53-59

- [6] T. Khayamian, M. Tabrizchi and M. T. Jafari; *Talanta*, 59, 2, (2003), 327-333
- [7] M.Tabrizchi, S.Shooshtari, *J. Chem. Thermodynamics* 35 (2003) 863-870
- [8] M.Tabrizchi, A.Abedi, *J. Phys. Chem. A*, 108, (2004), 6319-6324
- [9] M. A. Baim, R. L. Eatherton, and H. H. Hill, Jr., *Anal. Chem.* 55, (1983), 1761
- [10] C. S. Leasure, M. E. Fleischer, G. K. Anderson, and G. A. Eiceman, *Anal. Chem.* 58, (1986), 2142
- [11] H. Wohltzer, U.S. Patent Appl. US 581398, AO 3 August 1984
- [12] D. Wittmer, Y. H. Chen, B. K. Luckenbill, and H. H. Hill, Jr., *Anal. Chem.* 66, (1994), 2348
- [13] M.Tabrizchi, T.Khayamian and N.Taj, *Rev.Sci.Instrum.*, 71, 6, (2000), 2321-2328
- [14] M. M. Shahin, *J. Chem. Phys.* 45, 7 (1966) 2600-2605
- [15] G.A.Eiceman, E.G.Nazarov, J.E.Rodriguez, J.F.Bergloff *IJIMS* 1, 1, (1998), 28-37
- [16] Ch.J.Proctor, J.F.J.Todd *Org.M.Spect.* 18, 12 (1983) 509-516

<b>temperature</b>	20-58 °C	<b>E</b>	230 V.cm <sup>-1</sup>
<b>pressure</b>	101 kPa	<b>ΔU corona</b>	2 kV
<b>drift length</b>	8,3 cm	<b>drift gas flow</b>	0,8 l.min <sup>-1</sup>
<b>shutter opening time</b>	150-250 μs	<b>corona gas flow</b>	0-50 ml.min <sup>-1</sup>
<b>shutter opening period</b>	42 ms	<b>carrier gas flow</b>	0,4 l.min <sup>-1</sup>

Tab. 1: Conditions of the experiment

<b>Name</b>	<b>Formula</b>	<b>Structural formula</b>	<b>PA[eV]</b>
Acetone	C <sub>3</sub> H <sub>6</sub> O		8,42
Methanol	CH <sub>3</sub> OH		7,81
Ethanol	C <sub>2</sub> H <sub>5</sub> OH		8.05
Benzene	C <sub>6</sub> H <sub>6</sub>		7.78

Tab. 2: Measured organic compounds and corresponding proton affinities

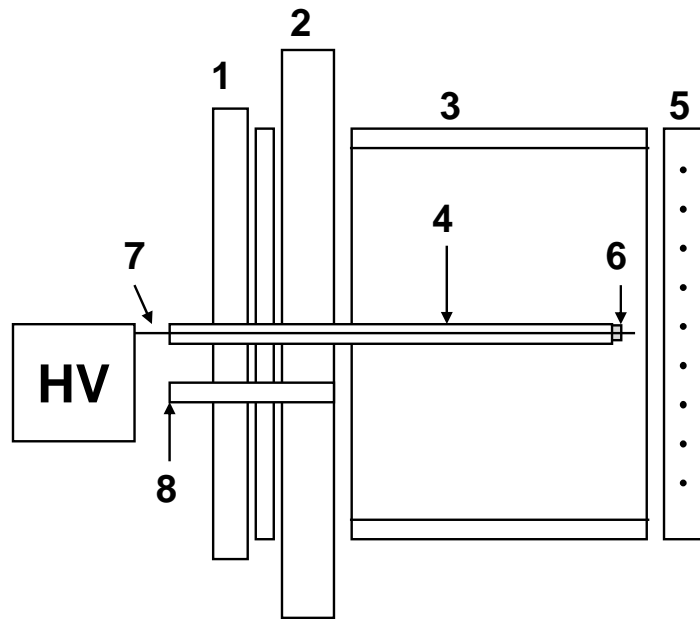


Fig. 1: Schematic view of the ionization source: 1-flange, 2-body of the apparatus, 3-teflon cylinder, 4-ceramic tube, 5-corona grid, 6-wire holder, 7-tungsten wire, 8-gas outlet

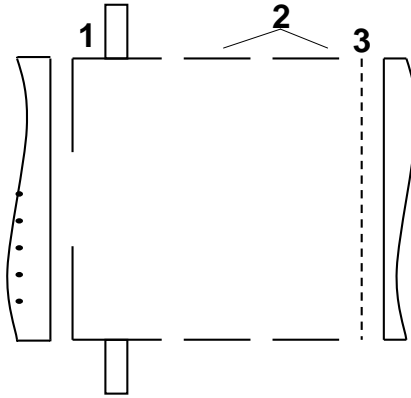


Fig. 2: Schematic view of the reaction region: (1) special electrode, (2) standard electrodes, (3) shutter grid

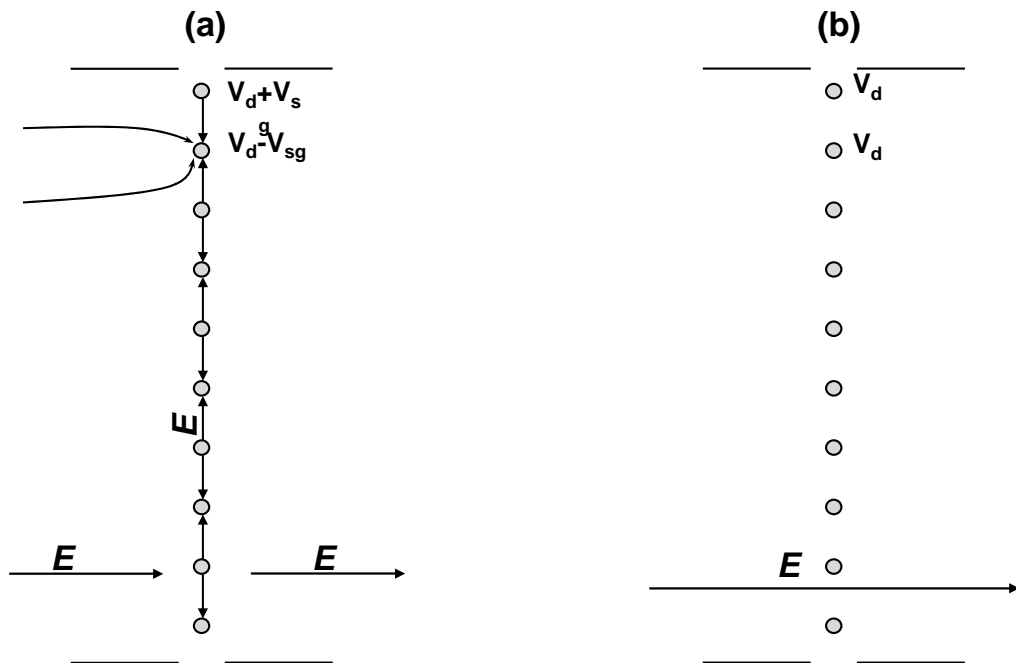


Fig. 3: Shutter grid (a) open, (b) closed

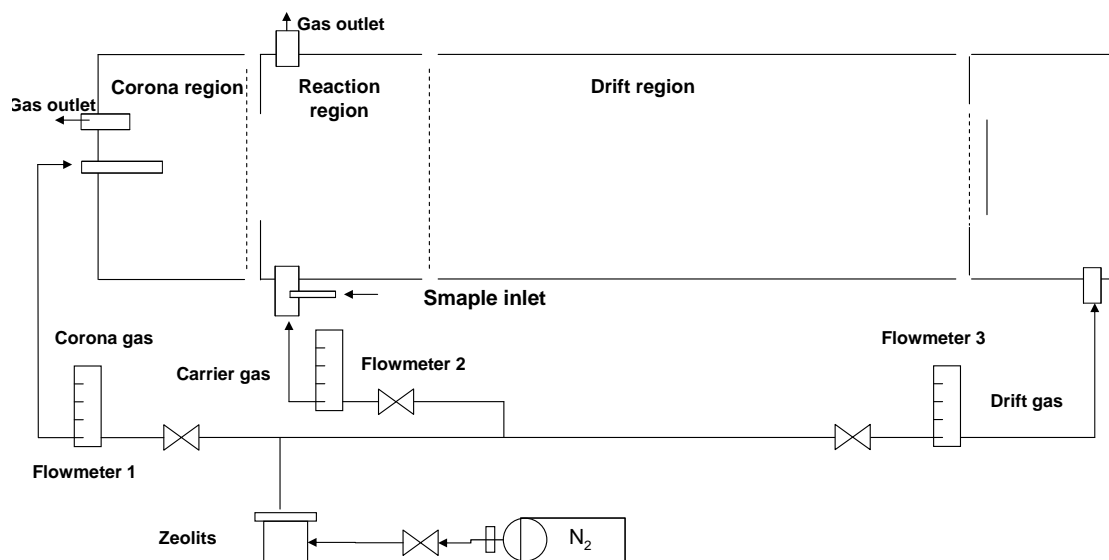


Fig. 4: Gas inlet system: Flowmeter no.1: 0-100 ml/min, Flowmeter no.2: 0-100 ml/min, Flowmeter no.3: 0,1-1,2l/min

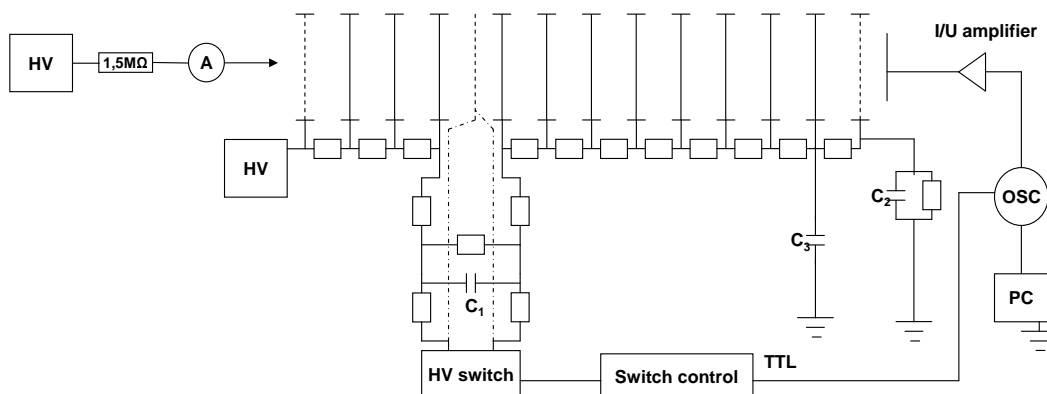


Fig. 5: The electrical circuits of the IMS

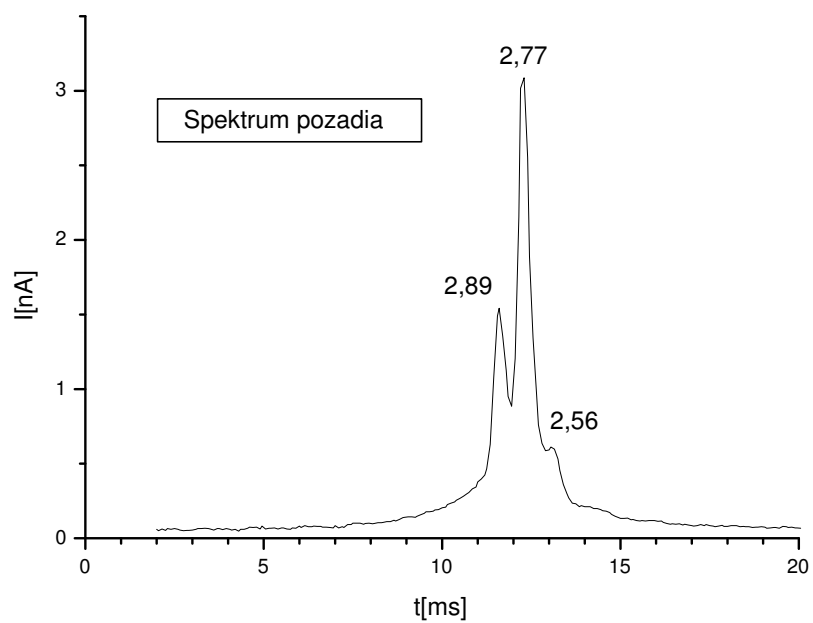


Fig. 6: The ion mobility spectrum of the primary ions (RIP - reactant ion peaks) and the corresponding reduced mobilities [ $\text{cm}^2 \cdot \text{V}^{-1} \cdot \text{s}^{-1}$ ]

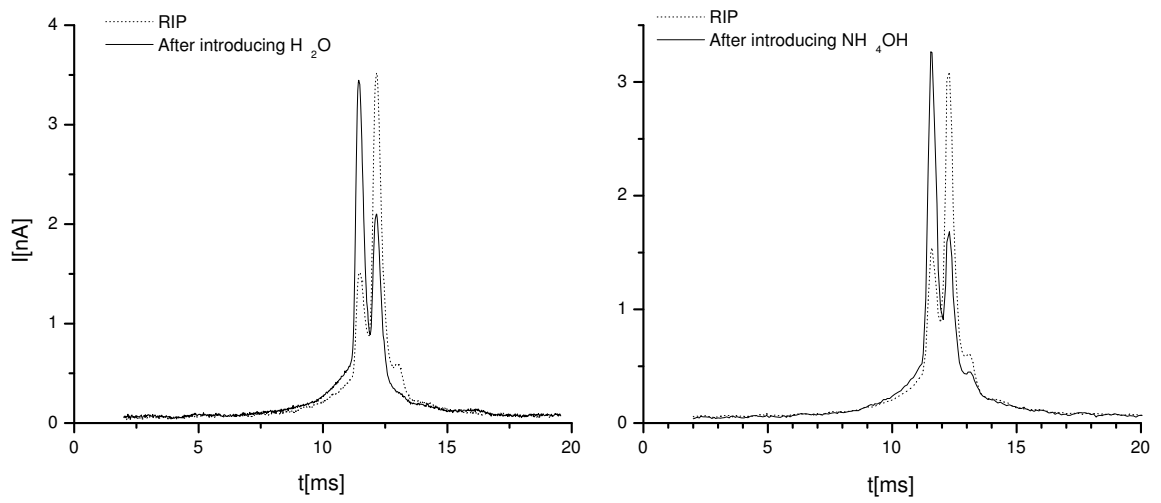


Fig. 7: The response of IMS on the introduction of the water and the ammonia into the discharge region

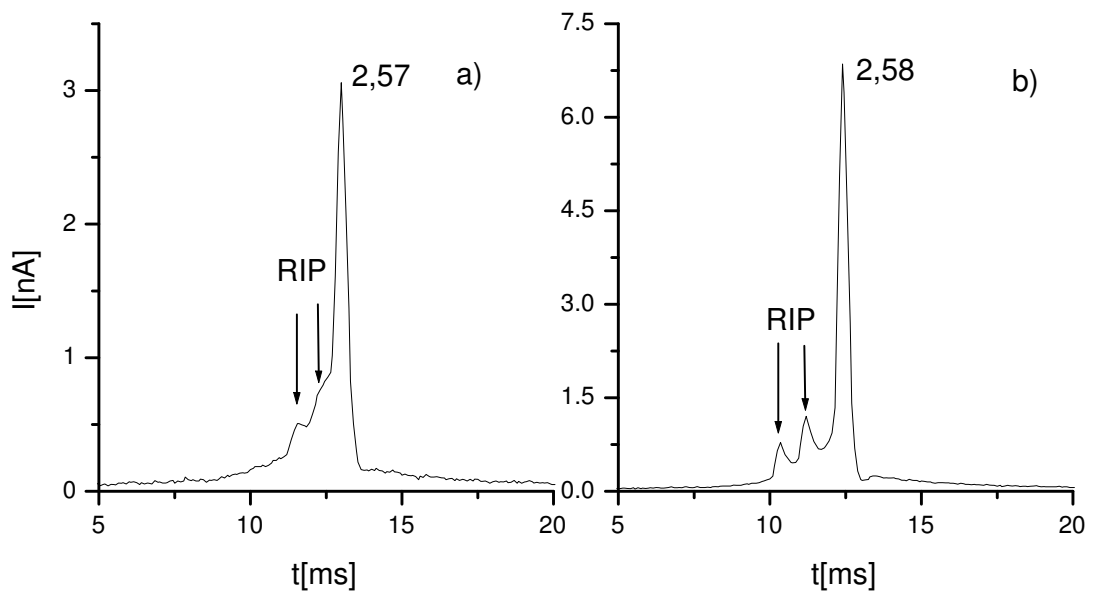


Fig. 8: Acetone: **a)** chemical ionization, **b)** ionization in the discharge

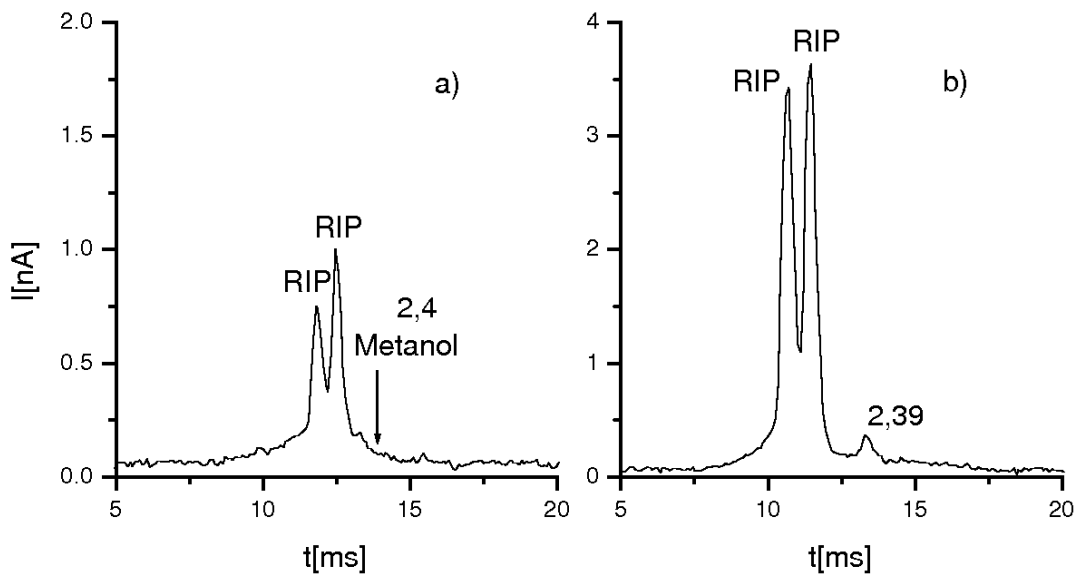


Fig. 9: Methanol: **a)** chemical ionization, **b)** ionization in the discharge

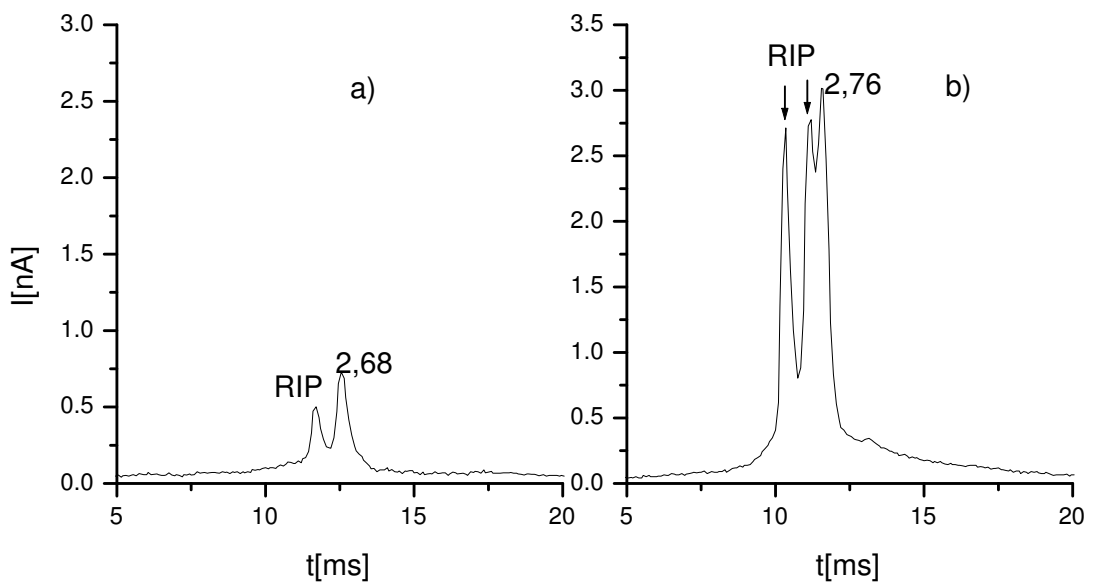


Fig. 10: Ethanol: **a)** chemical ionization, **b)** ionization in the discharge

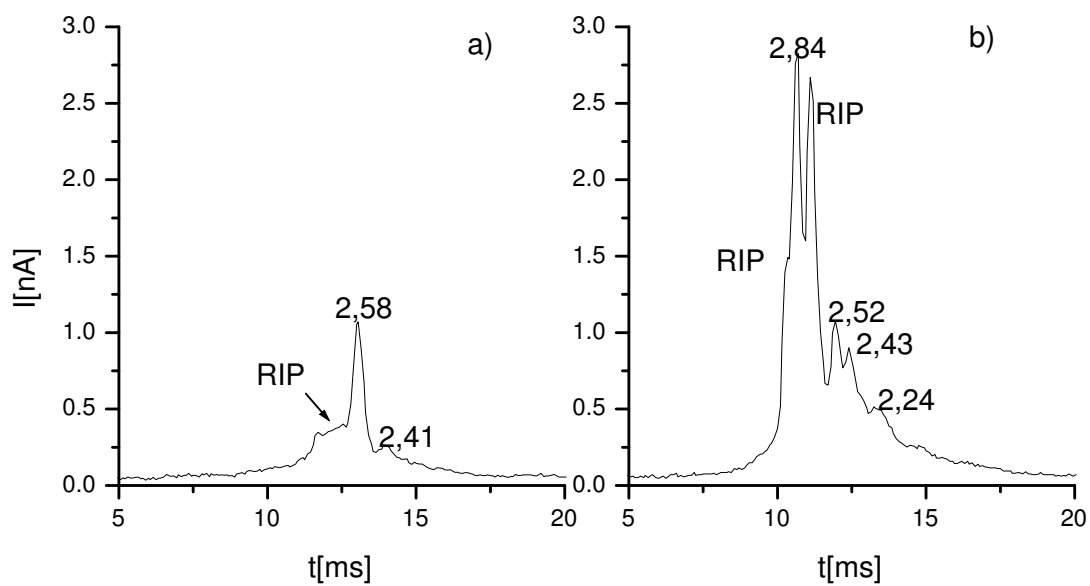


Fig. 11: Benzene: **a)** chemical ionization, **b)** ionization in the discharge